

## Supplementary Information

### Substitution of Copper Atoms into Defect-Rich Molybdenum Sulfide and their Electrocatalytic Activity

*Zixing Wang,<sup>a</sup> Harikishan Kannan,<sup>a</sup> Tonghui Su,<sup>a</sup> Jayashree Swaminathan,<sup>a</sup> Sharmila N. Shirodkar,<sup>a</sup> Francisco C Robles Hernandez,<sup>a,b</sup> Hector Calderon Benavides,<sup>c</sup> Robert Vajtai,<sup>a,d</sup> Boris I. Yakobson,<sup>a</sup> Ashokkumar Meiyazhagan,<sup>\*a</sup> Pulickel M. Ajayan<sup>\*a</sup>*

<sup>a</sup> Department of Materials Science and NanoEngineering, Rice University, Houston, TX 77005, USA.

Email: [ma37@rice.edu](mailto:ma37@rice.edu); [ajayan@rice.edu](mailto:ajayan@rice.edu)

<sup>b</sup> Department of Mechanical Engineering Technology, University of Houston, Houston, Texas 77204-4020, United States

<sup>c</sup> Departamento de Física, ESFM-IPN, Ed. 9, Instituto Politécnico Nacional UPALM, Mexico D.F., Mexico 07738

<sup>d</sup> Interdisciplinary Excellence Centre, Department of Applied and Environmental Chemistry, University of Szeged, Rerrich Béla tér 1, Szeged, H-6720, Hungary

## XPS Studies of MoS<sub>2-x</sub> synthesized using wet chemical approach

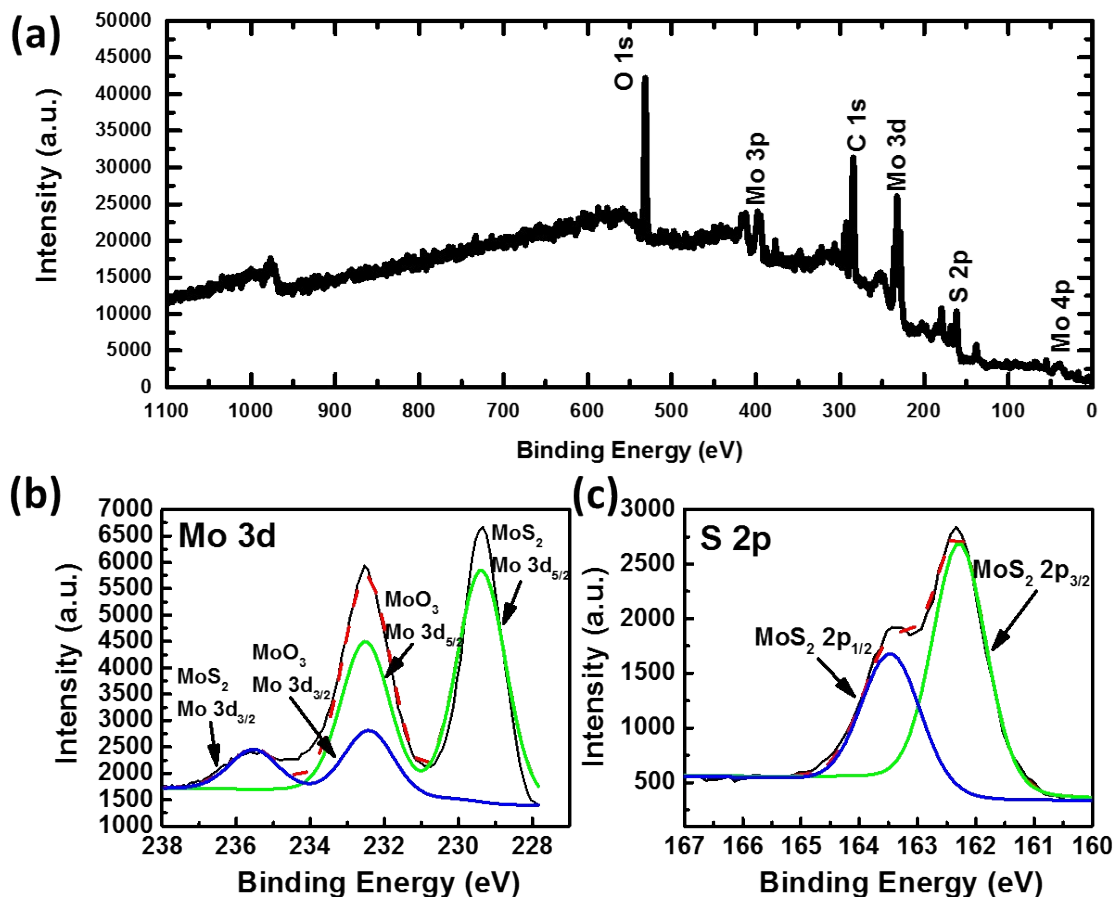


**Figure S1** XPS spectra of colloidal synthesized MoS<sub>2-x</sub> nanoparticles. (a) XPS survey spectra. The product contains 31.2 at% Mo, 37.5 at% S, and 31.2 at% O. (b) Mo 3d spectra of colloidal synthesized MoS<sub>2</sub> nanoparticles. Mo 3d<sub>5/2</sub> peak for MoS<sub>2</sub> and MoO<sub>3</sub> are located at 229.4 eV and 232.4 eV respectively. 78.1 at% of Mo comes from MoS<sub>2</sub> and 21.9 at% Mo comes from MoO<sub>3</sub>. (c) S 2p spectra of colloidal synthesized MoS<sub>2</sub> nanoparticles. The S intensity comes only from MoS<sub>2</sub>, where 2p<sub>3/2</sub> peak is located at 162.3 eV and 2p<sub>1/2</sub> peak is located at 163.5 eV.

## XPS Studies of $\text{MoS}_{1.99}\text{Cu}_{0.01}$ synthesized using wet chemical approach

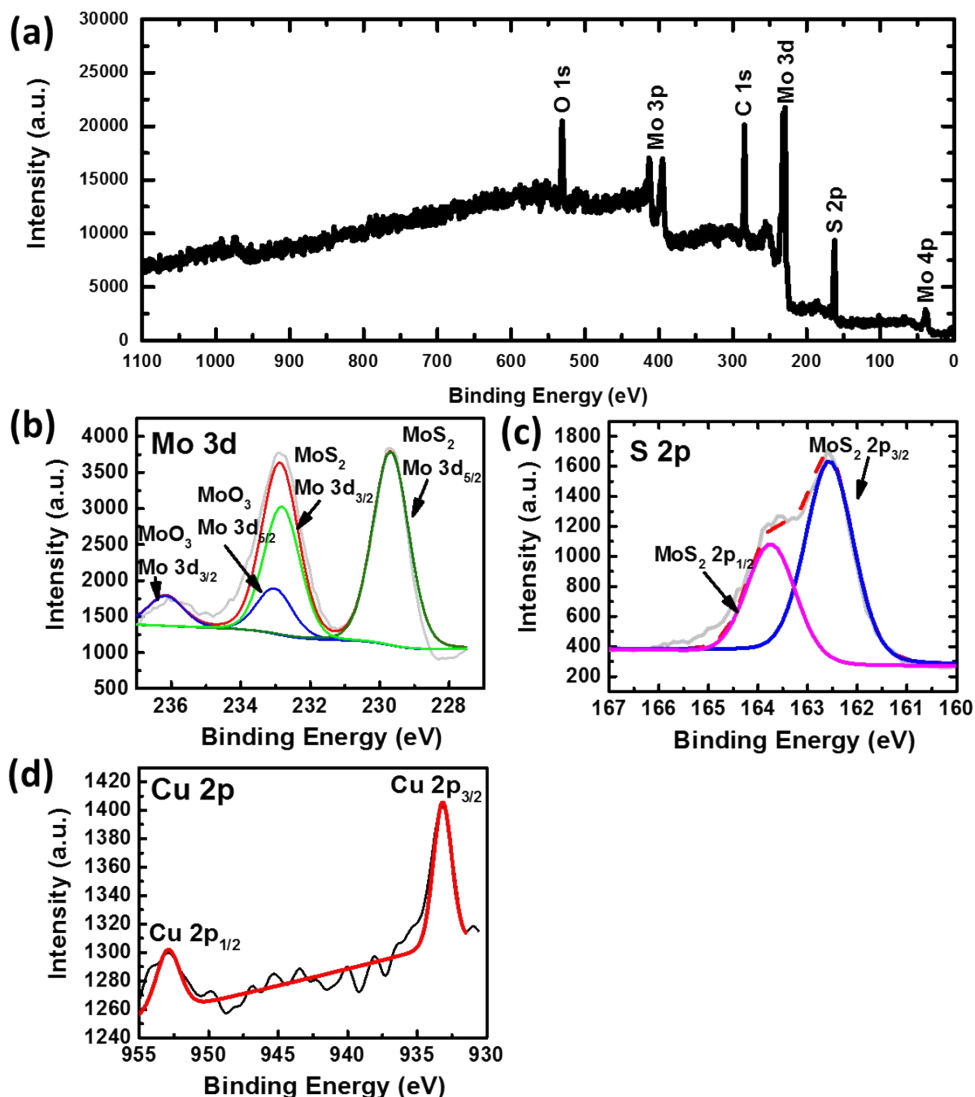


**Figure S2** XPS spectra of  $\text{MoS}_{1.99}\text{Cu}_{0.01}$  with tetrakis(acetonitrile)copper (I) hexafluorophosphate decomposed at 100 °C. (a) XPS survey spectra. The product contains 23.4 at% Mo, 33.7 at% S, 0.6 at% Cu and 42.3 at% O. (b) Mo 3d spectra of. Mo 3d<sub>5/2</sub> peak for MoS<sub>2</sub> and MoO<sub>3</sub> are located at 229.7 eV and 233.0 eV respectively. 61 at% of Mo comes from MoS<sub>2</sub> and 39 at% Mo comes from MoO<sub>3</sub>. (c) S 2p spectra of  $\text{MoS}_{1.99}\text{Cu}_{0.01}$ . The S intensity comes only from MoS<sub>2</sub>, where 2p<sub>3/2</sub> peak is located at 162.6 eV. (d) Cu 2p spectra of  $\text{MoS}_{1.99}\text{Cu}_{0.01}$ . The Cu signals come exclusively from Cu(0) or Cu(I). Since the Cu(0) and Cu(I) XPS peaks are close in position (< 0.1 eV difference in position), it is difficult to distinguish the two materials. The Cu 2p<sub>3/2</sub> peak is located at 933.3 eV.

## XPS Studies of $\text{MoS}_{1.9}\text{Cu}_{0.1}$ synthesized using wet chemical approach

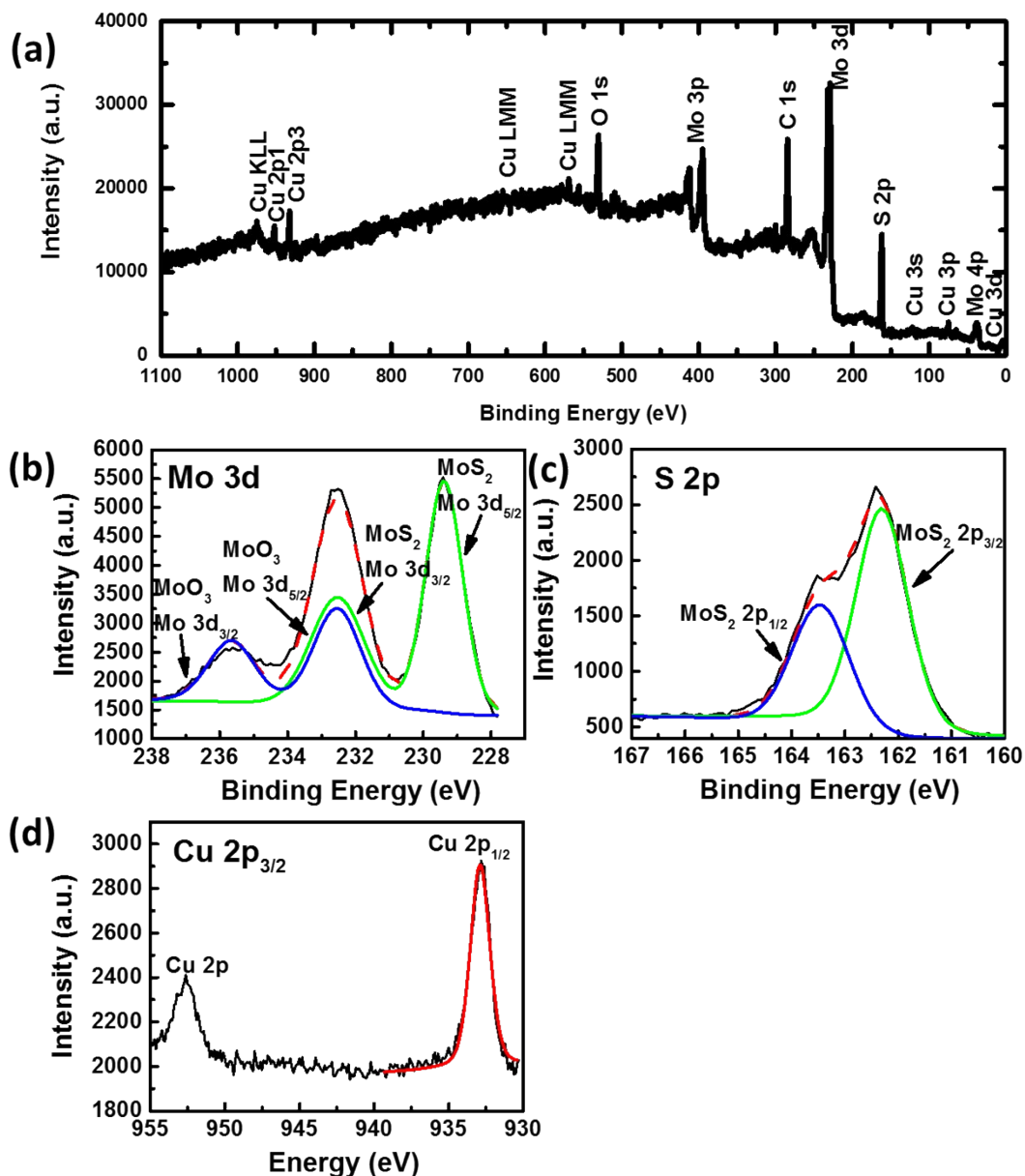


**Figure S3** XPS spectra of  $\text{MoS}_{1.9}\text{Cu}_{0.1}$  with tetrakis(acetonitrile)copper (I) hexafluorophosphate decomposed at 100 °C. (a) XPS survey spectra. The product contains 24.6 at% Mo, 35.6 at% S, 2.8 at% Cu and 37.0 at% O. (b) Mo 3d spectra of  $\text{MoS}_{1.9}\text{Cu}_{0.1}$ . Mo 3d<sub>5/2</sub> peak for MoS<sub>2</sub> and MoO<sub>3</sub> are located at 229.4 eV and 232.4 eV respectively. 82 at% of Mo comes from MoS<sub>2</sub> and 18 at% Mo comes from MoO<sub>3</sub>. (c) S 2p spectra of  $\text{MoS}_{1.9}\text{Cu}_{0.1}$ . The S intensity comes only from MoS<sub>2</sub>, where 2p<sub>3/2</sub> peak is located at 162.3 eV. (d) Cu 2p spectra of  $\text{MoS}_{1.9}\text{Cu}_{0.1}$ . The Cu 2p<sub>3/2</sub> peak for Cu(0) or Cu(I) is located at 932.9 eV.

## XPS Studies of MoS<sub>1</sub>Cu<sub>1</sub> synthesized using wet chemical approach

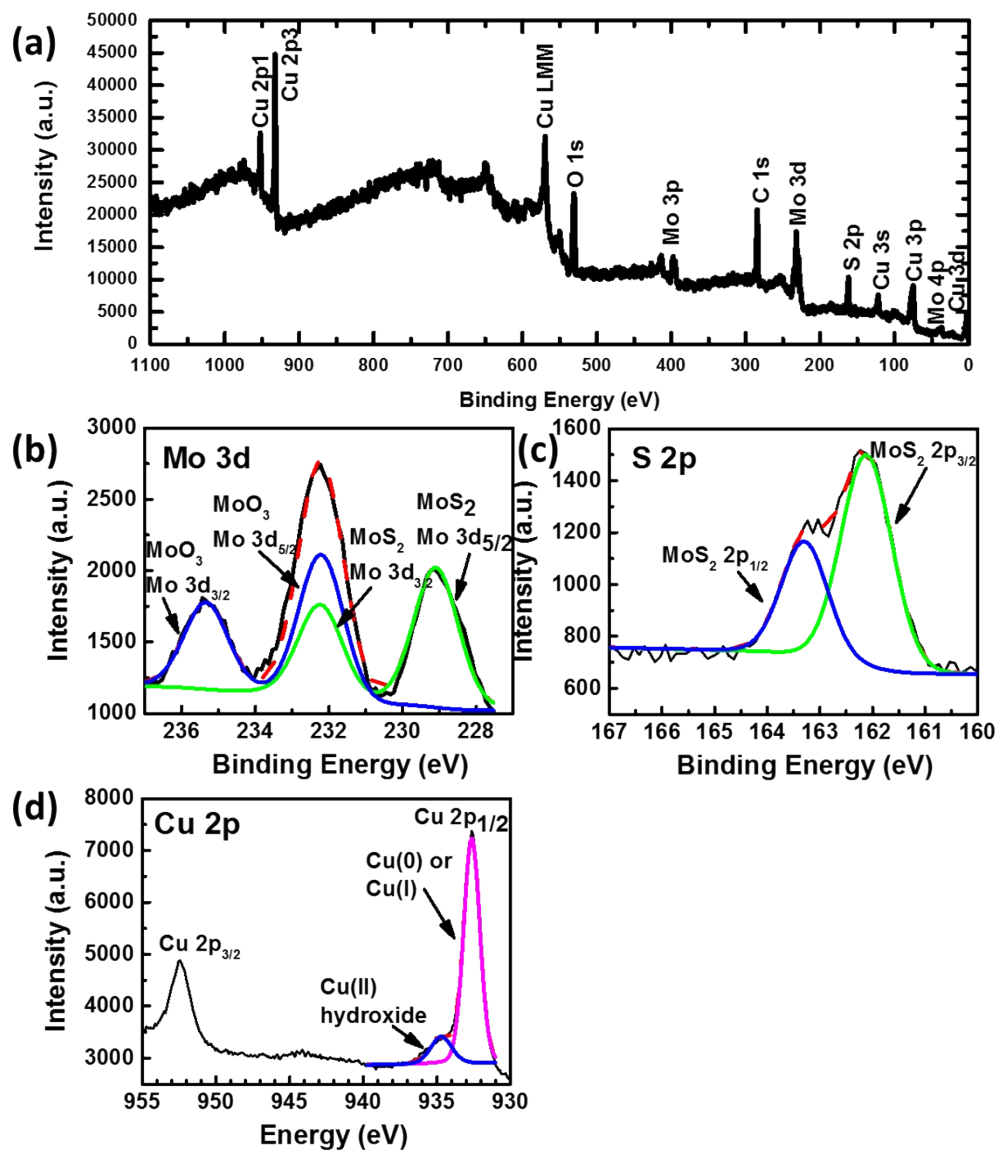


**Figure S4** XPS spectra of colloidal synthesized MoS<sub>1</sub>Cu<sub>1</sub> with tetrakis(acetonitrile)copper (I) hexafluorophosphate decomposed at 100 °C. (a) XPS survey spectra. The product contains 11.0 at% Mo, 15.7 at% S, 19.8 at% Cu and 53.5 at% O. (b) Mo 3d spectra. Mo 3d<sub>5/2</sub> peak for MoS<sub>2</sub> and MoO<sub>3</sub> are located at 229.1 eV and 232.2 eV respectively. 51 at% of Mo comes from MoS<sub>2</sub> and 49 at% Mo comes from MoO<sub>3</sub>. (c) S 2p spectra of MoSCu. The S intensity comes only from MoS<sub>2</sub>, where 2p<sub>3/2</sub> peak is located at 162.1 eV. (d) Cu 2p spectra of MoSCu. The Cu signals come from Cu(0) or Cu(I), and Cu(II) hydroxide. The Cu 2p<sub>3/2</sub> peak for Cu(0) or Cu(I) is located at 932.6 eV

and for Cu(II) hydroxide is located at 934.7 eV. The Cu contains 86 at% Cu(0) or Cu(I) and 14 at% Cu(II) hydroxide.

### XPS Studies of $\text{MoS}_1\text{Cu}_1$ synthesized using wet chemical approach

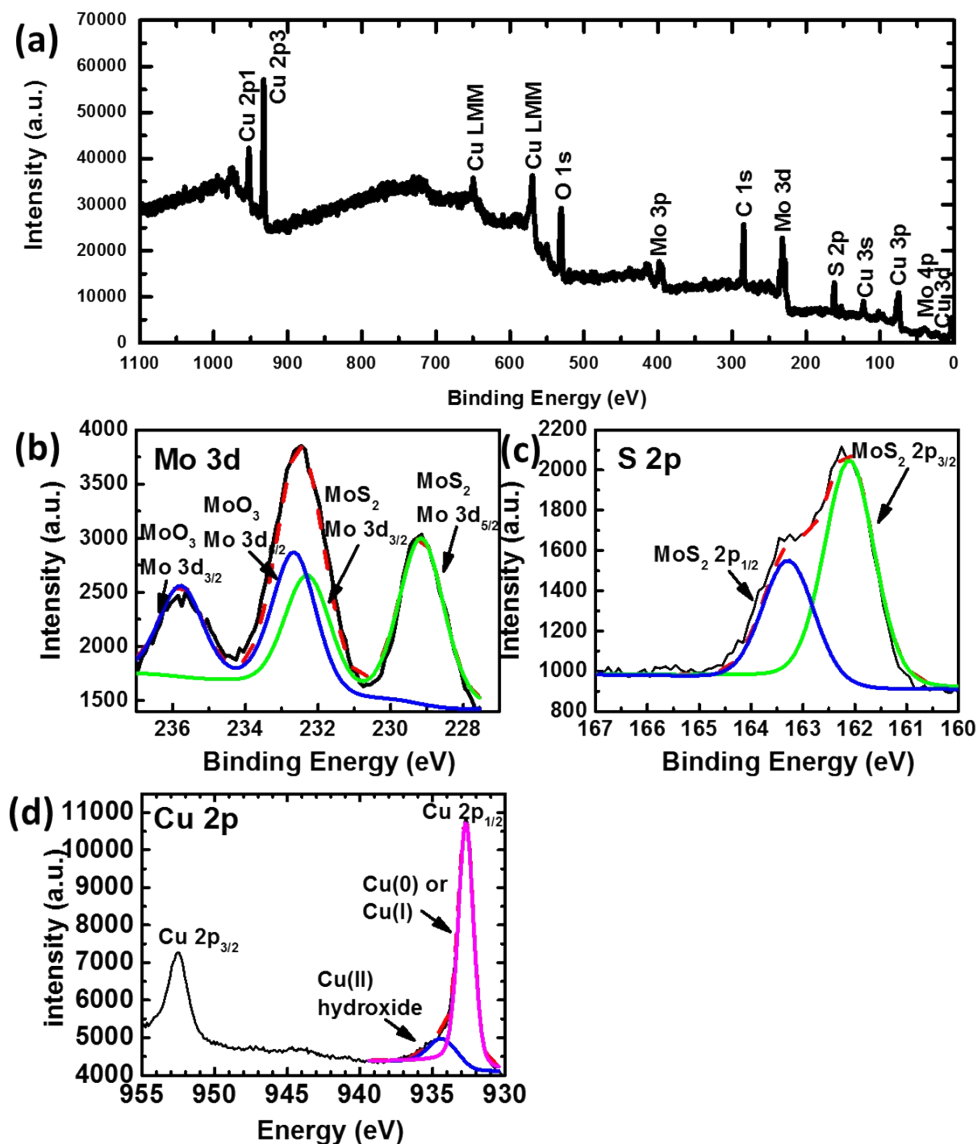


**Figure S5** XPS spectra of colloidal synthesized  $\text{MoS}_1\text{Cu}_1$  with tetrakis(acetonitrile)copper (I) hexafluorophosphate decomposed at 200 °C. (a) XPS survey spectra. The product contains 12.1 at% Mo, 16.3 at% S, 18.6 at% Cu and 53.0 at% O. (b) Mo 3d spectra of  $\text{MoS}_1\text{Cu}_1$ . Mo  $3d_{5/2}$  peak for  $\text{MoS}_2$  and  $\text{MoO}_3$  are located at 229.2 eV and 232.6 eV respectively. 56 at% of Mo comes from  $\text{MoS}_2$  and 44 at% Mo comes from  $\text{MoO}_3$ . (c) S2p spectra of  $\text{MoS}_1\text{Cu}_1$ . The S intensity is due to

MoS<sub>2</sub>, where 2p<sub>3/2</sub> peak is located at 162.2 eV. (d) Cu 2p spectra. The Cu signals display Cu(0) or Cu(I), and Cu(II) hydroxide. The Cu 2p<sub>3/2</sub> peak for Cu(0) or Cu(I) is located at 933.3 eV and Cu(II) hydroxide is located at 935.5 eV. The Cu contains 76 at% Cu(0) or Cu(I) and 24 at% Cu(II) hydroxide.

### TEM observation of the MoS<sub>1.99</sub>-Cu<sub>0.01</sub>

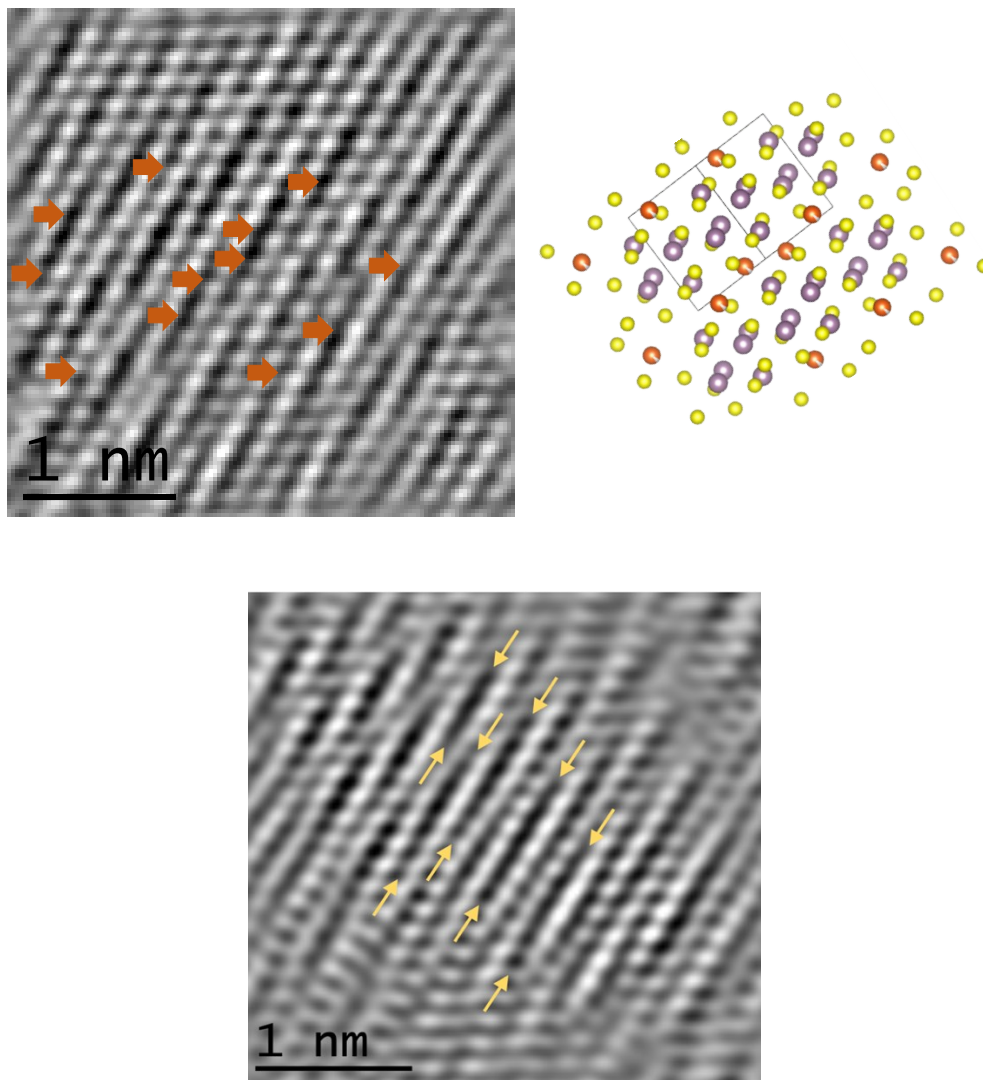


**Figure S6** TEM observation of the MoS<sub>1.99</sub>-Cu<sub>0.01</sub>. Scheme: S (yellow), Mo (purple), Cu (orange) showing spaces in between the layers. The observed gaps are due to the presence of copper atoms.

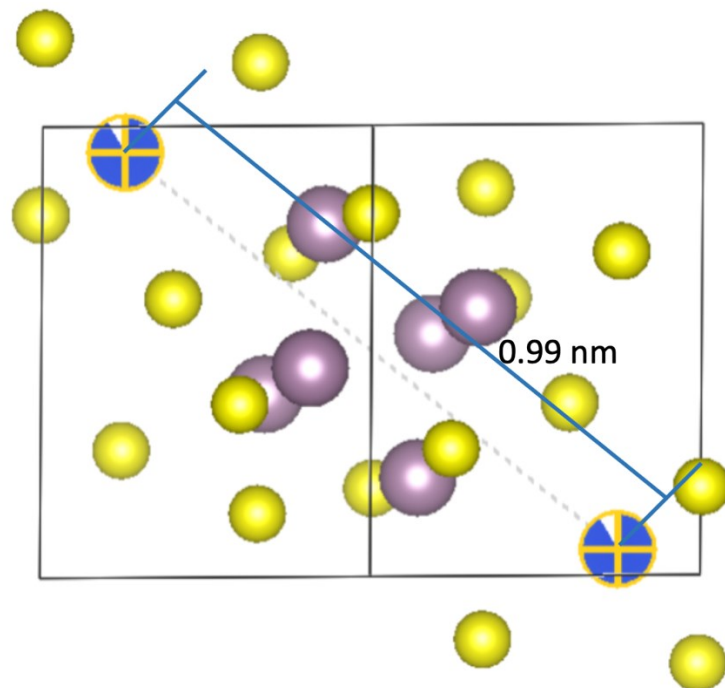


**Figure S7** The measured distance between the Cu atoms is approximately 0.994 nm.

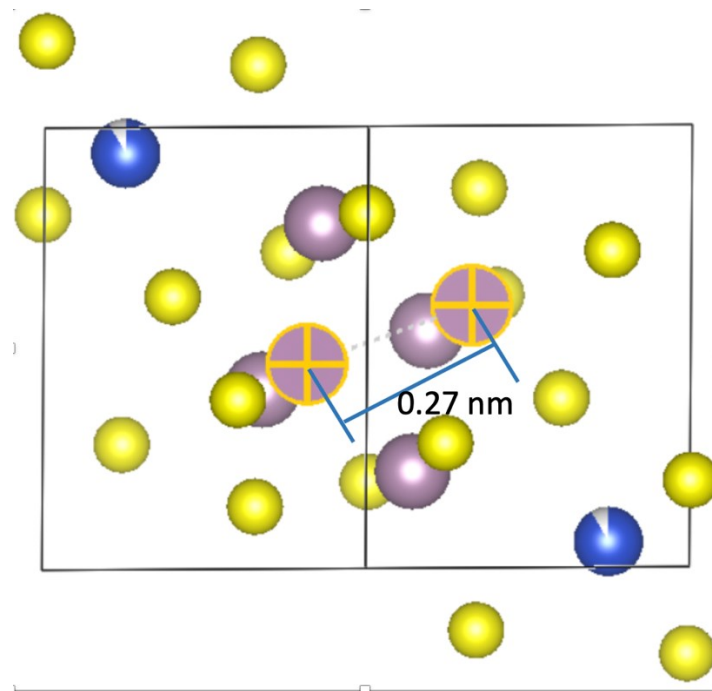


**Figure S8** The measured Mo-S-Mo atoms is approximately 0.27 nm.

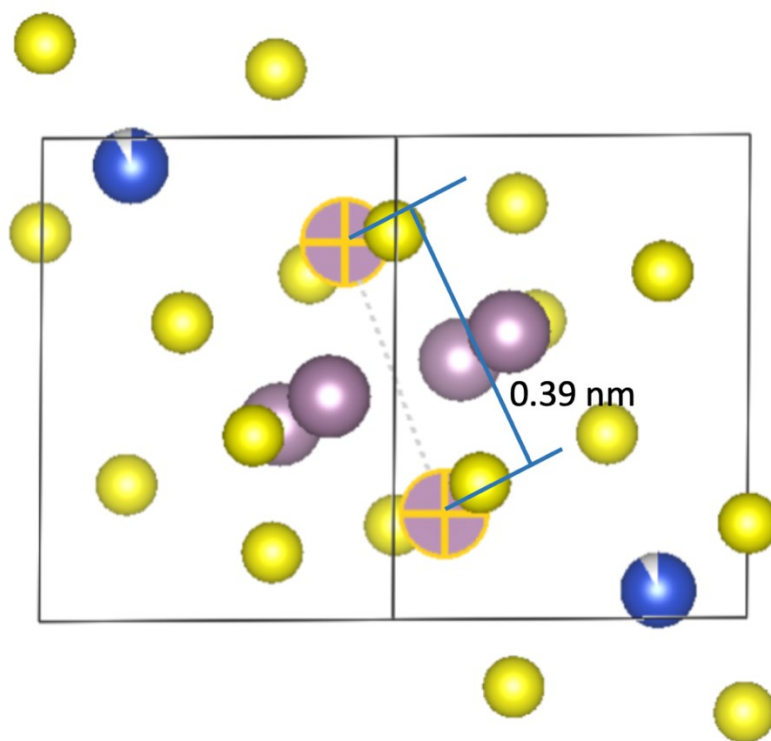


**Figure S9** The measured S-Mo-S atoms is approximately 0.39 nm.

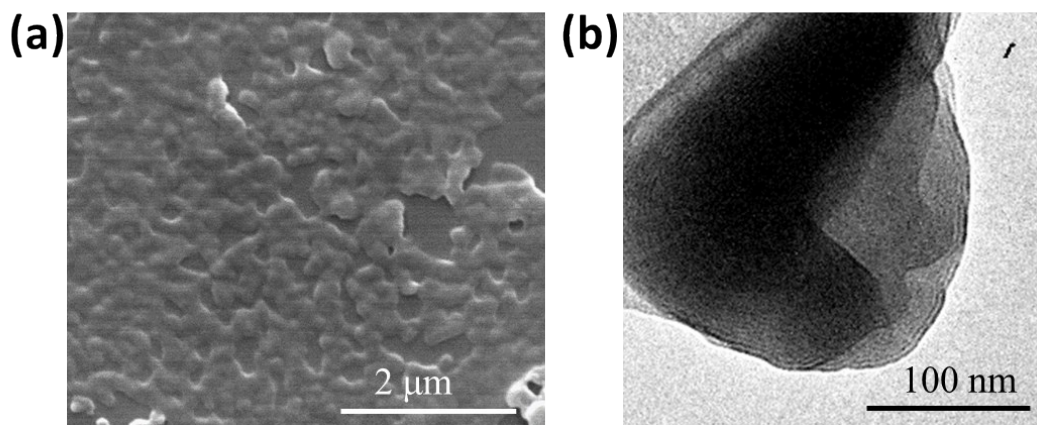


**Figure S10** (a) SEM image of the  $\text{MoS}_{1.99}\text{Cu}_{0.01}$  on Si wafer. A continuous thin layer of sheets can be observed. (b) TEM image of  $\text{MoS}_{1.99}\text{Cu}_{0.01}$  displaying layered crystalline structure at the edges of the cluster.

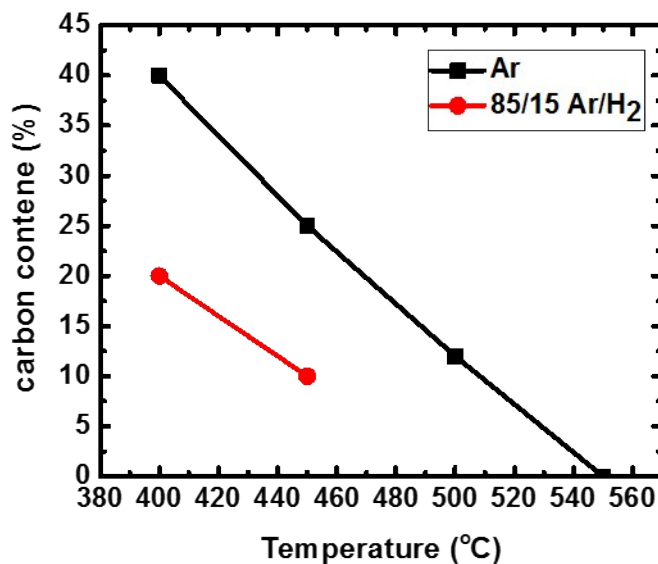


**Figure S11** carbon content in the Cu doped  $\text{MoS}_2$  samples when annealed in either Ar or 85/15 vol/vol Ar/H<sub>2</sub> atmosphere at temperatures ranging from 400 °C to 550 °C for 30 mins. The carbon content is determined by EDS. Ar/H<sub>2</sub> is more effective in removing the carbon from the sample. However, caution should be taken since the H<sub>2</sub> will reduce  $\text{MoS}_2$  nanosheets and produce defects in the material. All carbon content can be removed at 550 °C under Ar atmosphere.

Effect of temperature and increase in proportion of copper precursor in formation of  $\text{MoS}_{1.99}\text{Cu}_{0.01}$

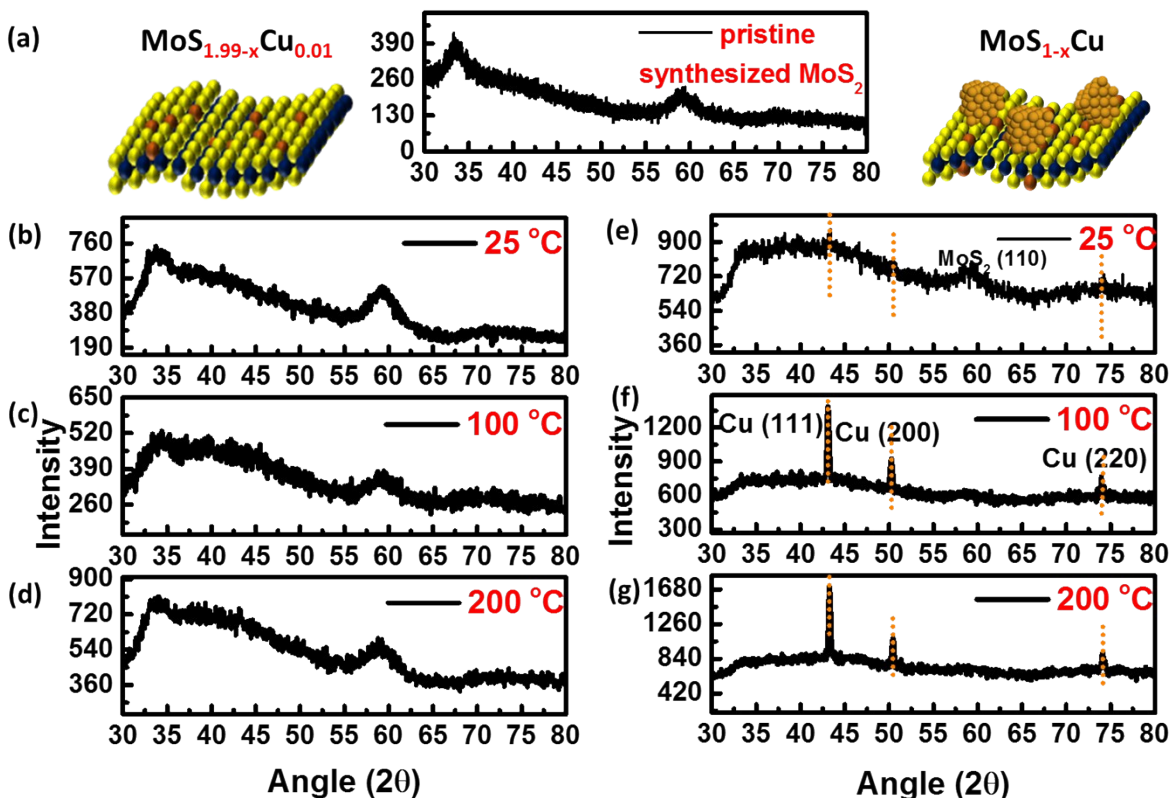


**Figure S12** XRD spectra of (a) colloidal synthesized  $\text{MoS}_2$ . Left inset: cartoon of expected structure of  $\text{MoS}_{1.99}\text{Cu}_{0.01}$ . Right inset: cartoon of expected structure of  $\text{MoS}_{1.99}\text{Cu}$ . (b – d)  $\text{MoS}_{1.99}\text{Cu}_{0.01}$  with tetrakis(acetonitrile)copper (I) hexafluorophosphate decomposed at (b) 25 °C, (c) 100 °C, and (d) 200 °C. The faint peak observed at 43.25° corresponds to the prominent peak of Cu crystal. However, due to low Cu concentration, the Cu XRD peaks are faint. (e – g)  $\text{MoS}_{1-x}\text{Cu}$  with tetrakis(acetonitrile)copper (I) hexafluorophosphate decomposed at (e) 25 °C, (f) 100 °C, and (g) 200 °C.

Distinct peaks of Cu crystal observed from samples synthesized at 100 °C, and 200 °C imply an optimal tetrakis(acetonitrile)copper (I) hexafluorophosphate decomposition temperature between 100-200 °C. The sharp peaks of Cu (marked by orange dashed lines, PDF # 00-026-1116) indicate the Cu crystals in the sample are highly crystalline, making the  $\text{MoS}_2$  nanostructures faint in comparison.

### Reaction pathway for synthesis of Cu doped MoS<sub>x</sub>

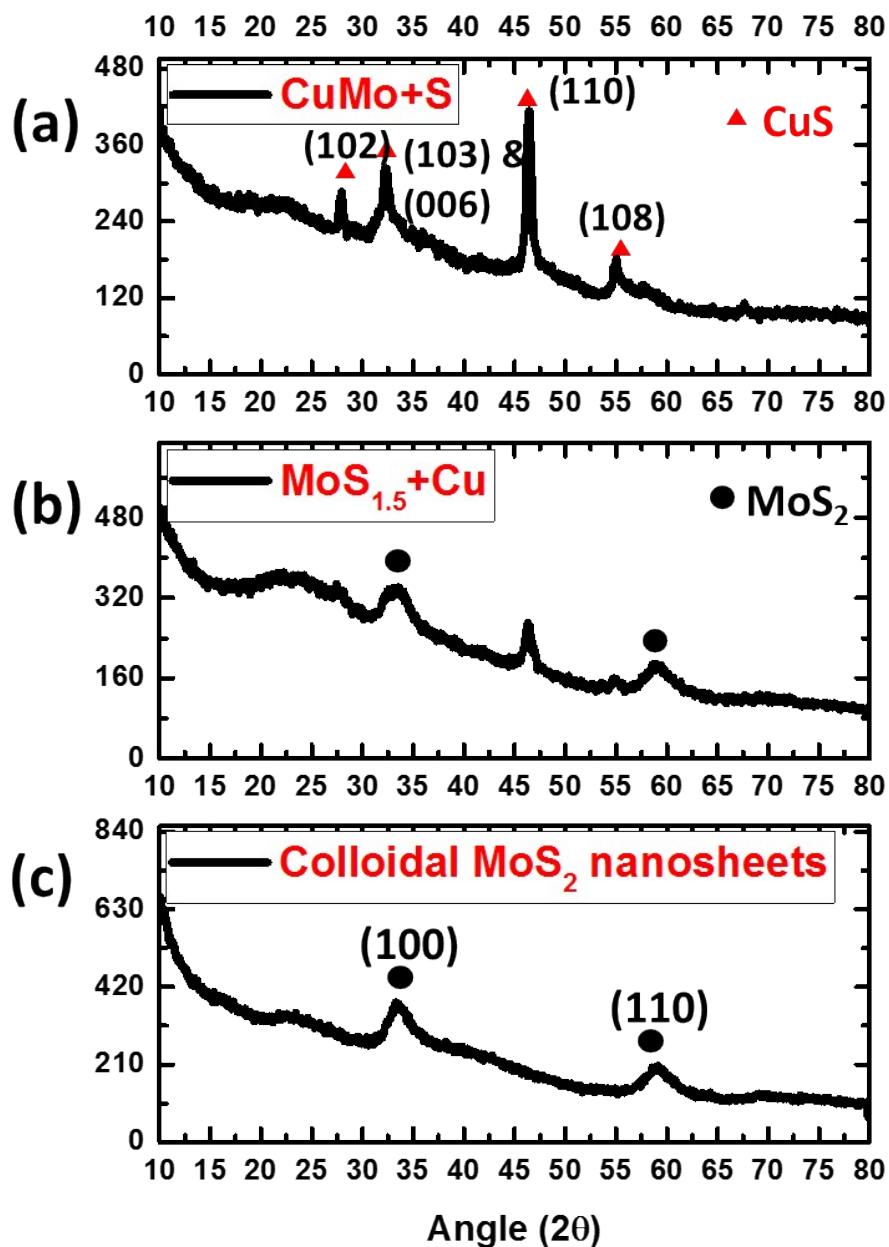


**Figure S13** XRD spectra of Cu, Mo, S synthesized under different conditions at 300 °C. (a) tetrakis(acetonitrile)copper (I) hexafluorophosphate was added to Mo-OAM at 1:1 molar ratio at 150 °C and reacted for 30 minutes. Then S-ODE was added to Cu, Mo-OAM solution and reacted at 300 °C. Distinct CuS peaks are observed from the spectra. This indicates a kinetically favored reaction between Cu and S to form CuS than MoS<sub>2</sub>. Thus, it is necessary to create a stable MoS<sub>2</sub> structure before Cu can be added to the reaction. (b) A 1 mole of tetrakis(acetonitrile)copper (I) hexafluorophosphate was added to synthesize 1 mol of MoS<sub>1.5</sub> at 300°C. Other than the spectra

from MoS<sub>2</sub> nanoparticles, peaks corresponding to CuS is also observed, signifying, the thermal activation energy is sufficient to form CuS compound at 300 °C. (c) XRD spectra corresponding to MoS<sub>2-x</sub> nanosheets synthesized through colloidal synthesis.

#### Raman studies of MoS<sub>1.99</sub>Cu<sub>0.01</sub> synthesized at different temperature

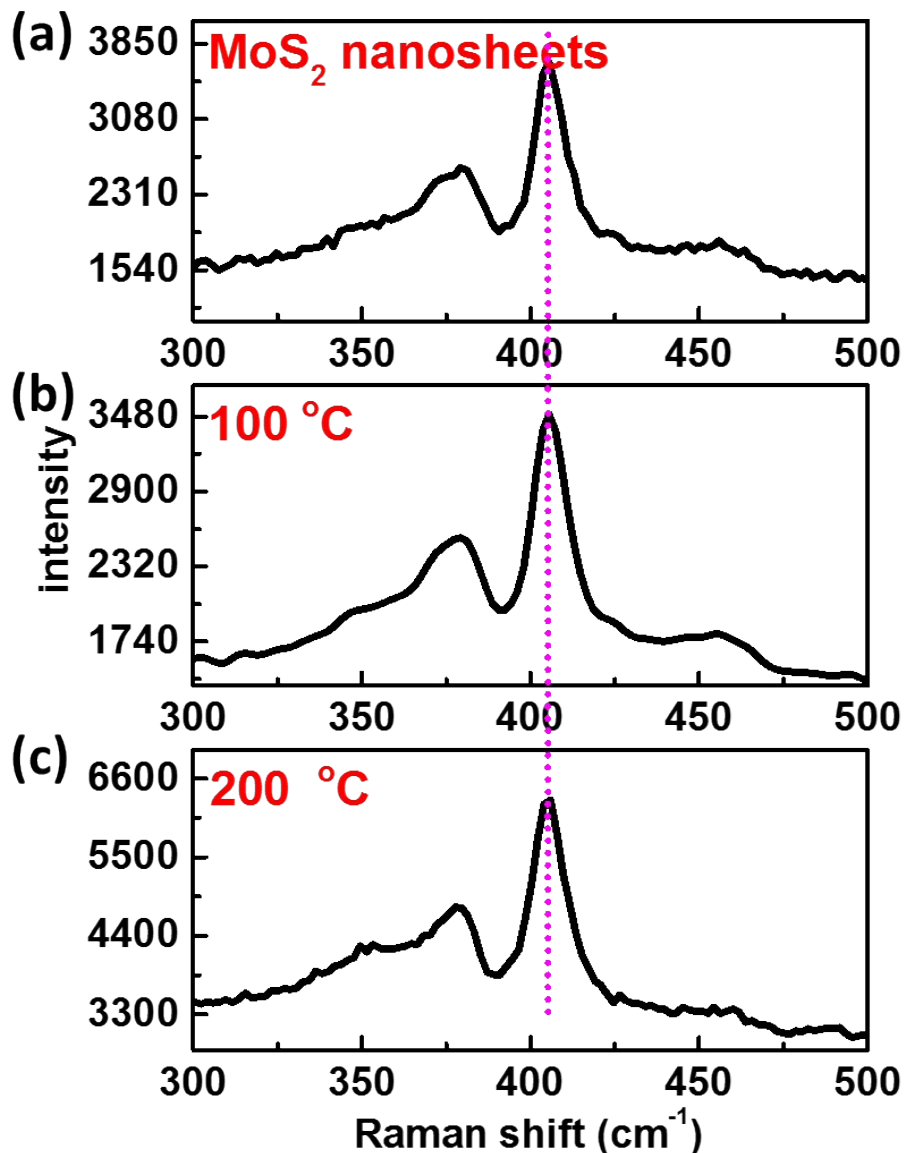


**Figure S14** Raman spectra of (a) colloidal synthesized MoS<sub>2-x</sub> and (b-c) MoS<sub>1.99</sub>Cu<sub>0.01</sub> with tetrakis(acetonitrile)copper (I) hexafluorophosphate decomposed at (b) 100 °C, and (c) 200 °C. The A<sub>1g</sub> peak from (a), (b), and (c) are seen at 405.82, 405.80, and 405.74 cm<sup>-1</sup> respectively.

Raman studies of  $\text{MoS}_{1.9}\text{Cu}_{0.1}$  synthesized at different temperature

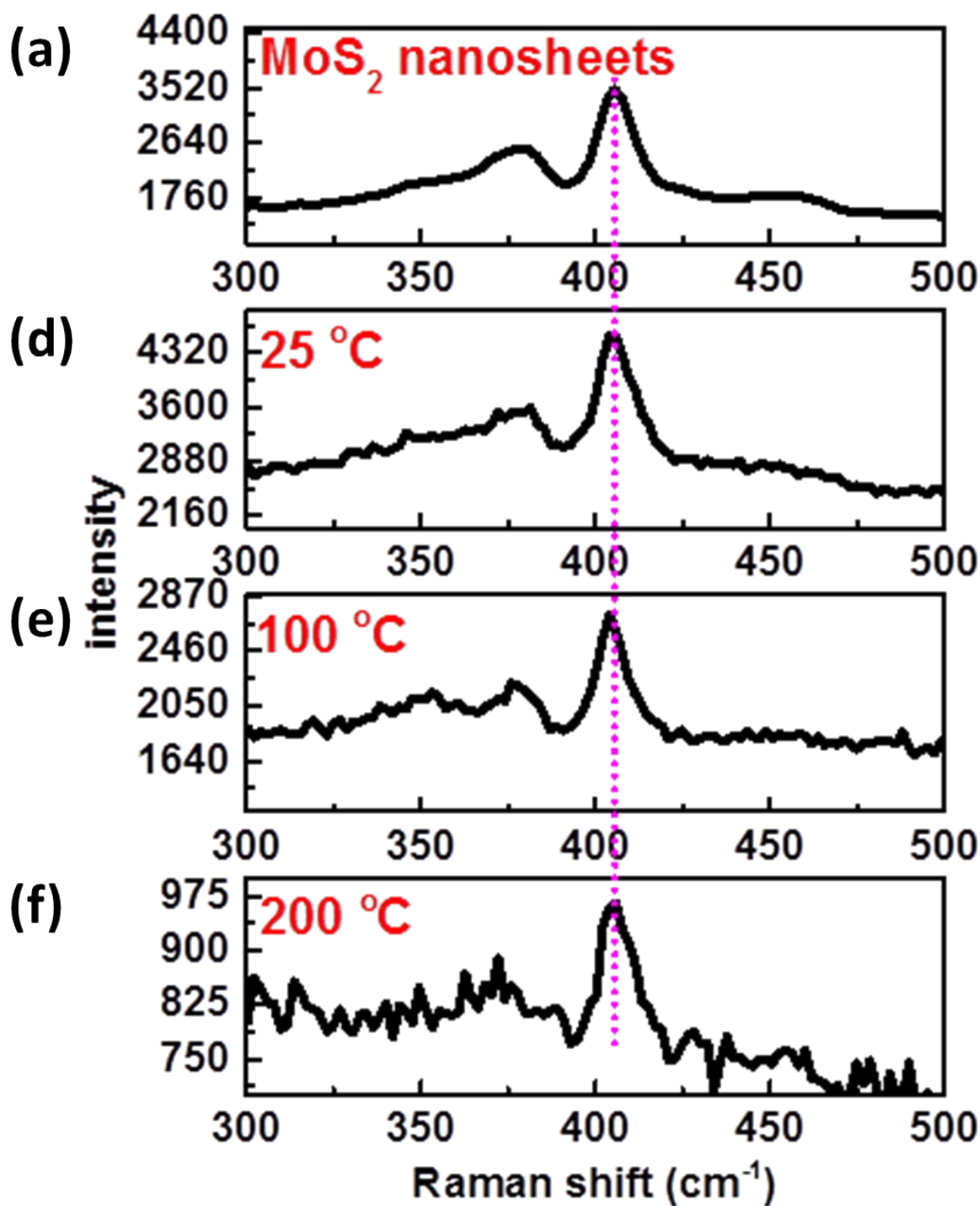


**Figure S15** Raman spectra of (a) colloidal synthesized  $\text{MoS}_{2-x}$  and (b-d)  $\text{MoS}_{1.9}\text{Cu}_{0.1}$  with tetrakis(acetonitrile)copper (I) hexafluorophosphate decomposed at (b) 25 °C, (c) 100 °C, and (d) 200 °C.

### Raman studies of $\text{MoS}_1\text{Cu}_1$ synthesized at different temperature

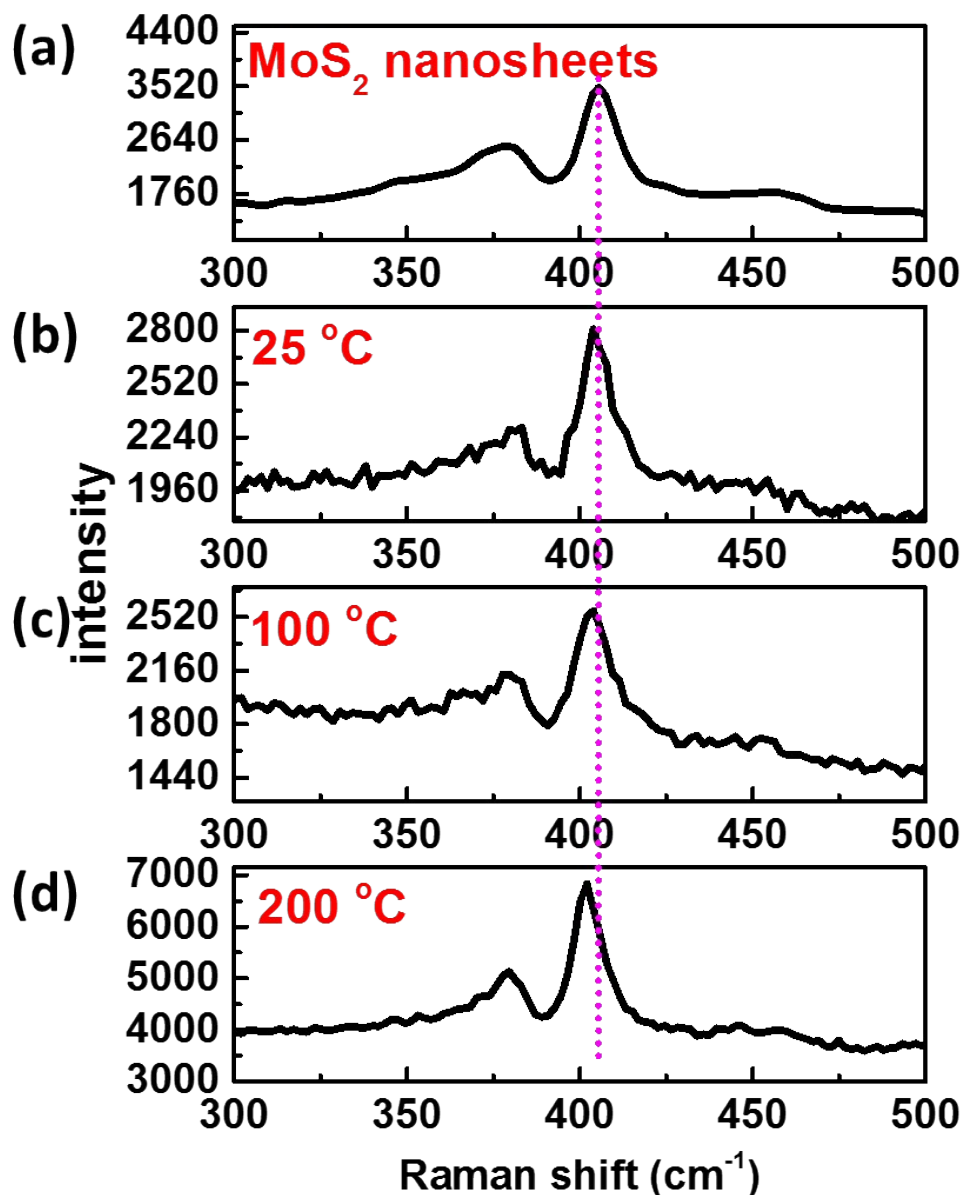


**Figure S16** Raman spectra of colloidal synthesized (a)  $\text{MoS}_{2-x}$  nanostructures, (b-d)  $\text{MoS}_1\text{Cu}_1$  with tetrakis(acetonitrile)copper (I) hexafluorophosphate decomposed at (b)  $25^\circ\text{C}$ , (c)  $100^\circ\text{C}$ , and (d)  $200^\circ\text{C}$ .  $\text{A}_{1\text{g}}$  peak position for synthesized  $\text{MoS}_2$  nanostructures is  $405.80\text{ cm}^{-1}$ . The peak position for tetrakis(acetonitrile)copper (I) hexafluorophosphate decomposed at  $25^\circ\text{C}$  is  $404.86\text{ cm}^{-1}$ , at  $100^\circ\text{C}$  is  $403.90\text{ cm}^{-1}$ , and at  $200^\circ\text{C}$  is  $402.40\text{ cm}^{-1}$ . A total shift of  $3.4\text{ cm}^{-1}$  occurred upon Cu addition at  $200^\circ\text{C}$ .

## SEM EDAX observation of synthesized nanoparticles

EDAX observation of MoS<sub>2-x</sub> nanostructures

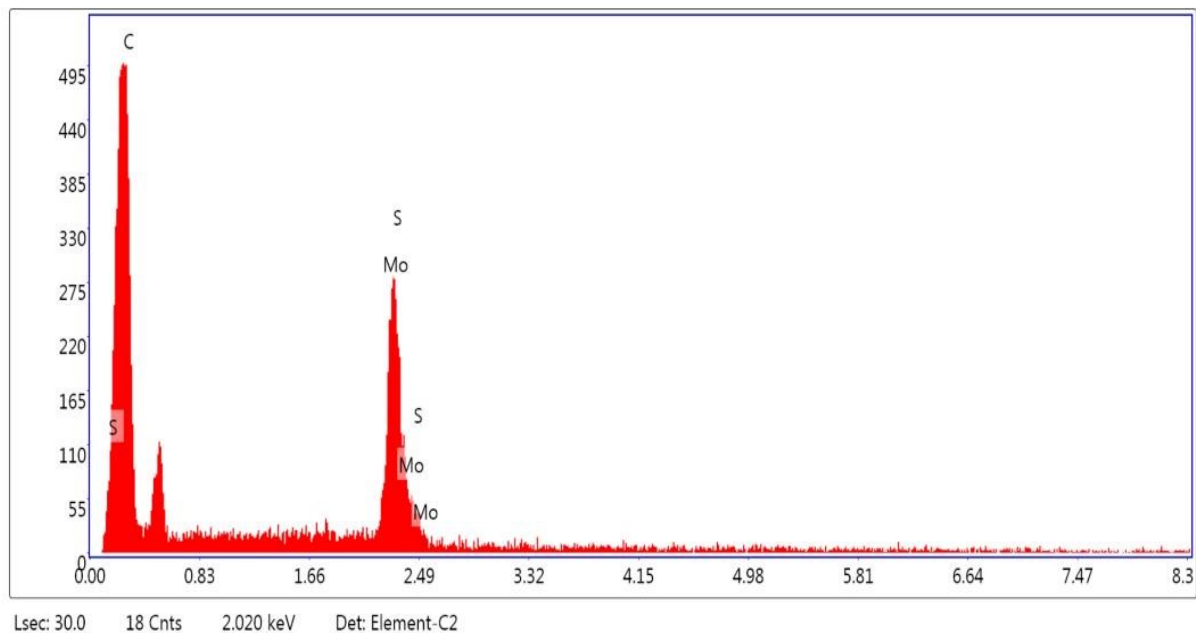


**Figure S17** EDAX analysis of MoS<sub>2-x</sub> sample shows presence of Molybdenum and sulfur

## Formation of Cu doped MoS at 100°C

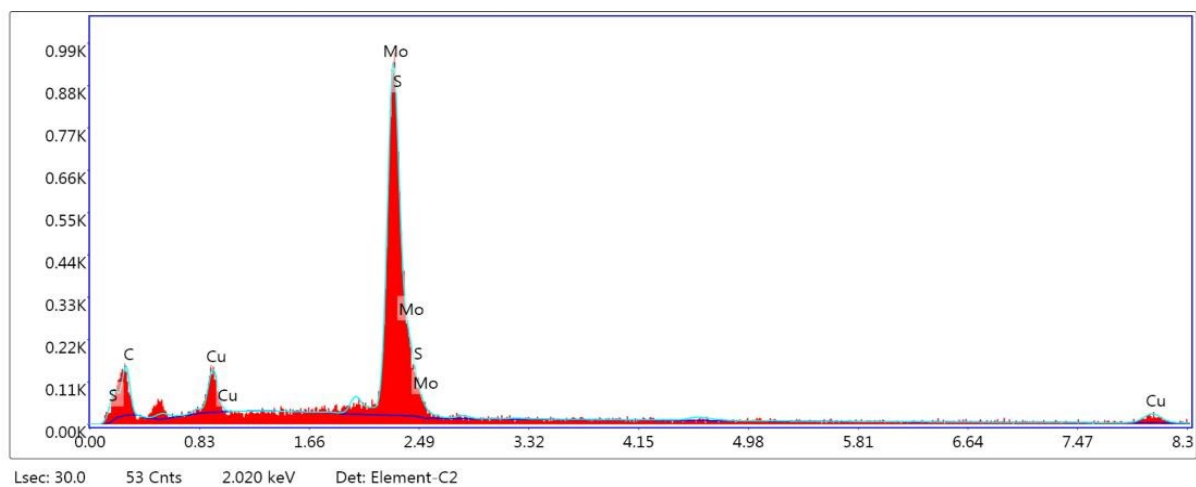


**Figure S18** EDAX analysis of Cu doped MoS<sub>2-x</sub> synthesized at 100°C shows presence of Molybdenum, copper and sulfur

### Formation of CuS at 300°C

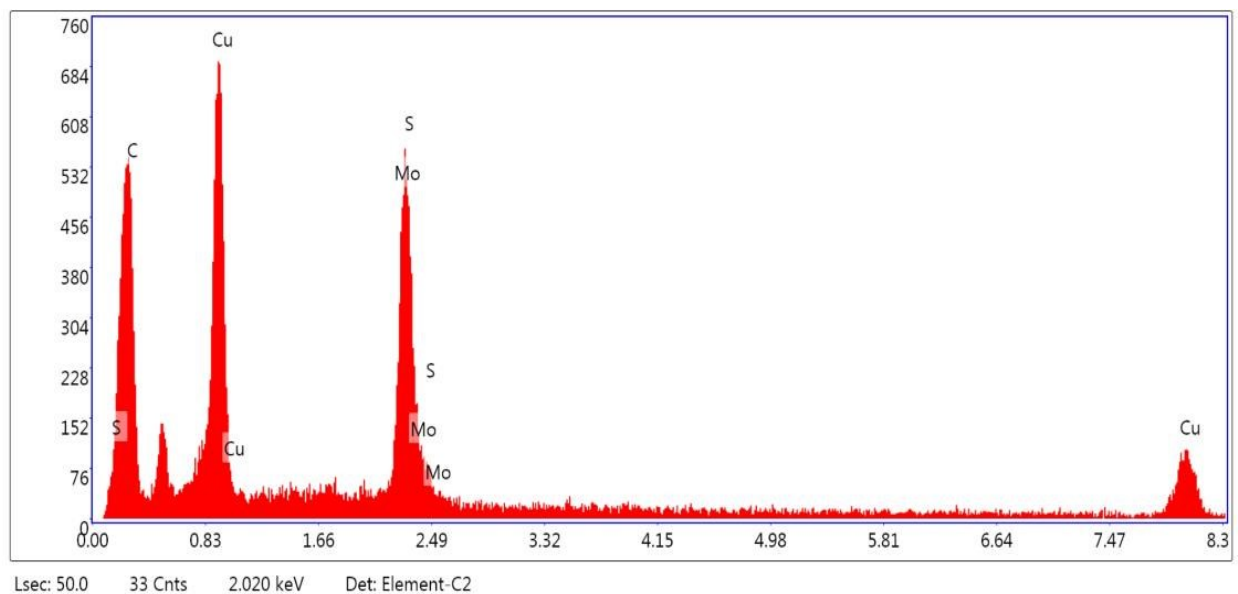


**Figure S19** EDAX analysis of Cu doped  $\text{MoS}_{2-x}$  synthesized at 300°C displays presence of Molybdenum, along with higher percentages of sulfur and copper.

PL studies of  $\text{MoS}_{1.99}\text{Cu}_{0.01}$  synthesized at different temperature

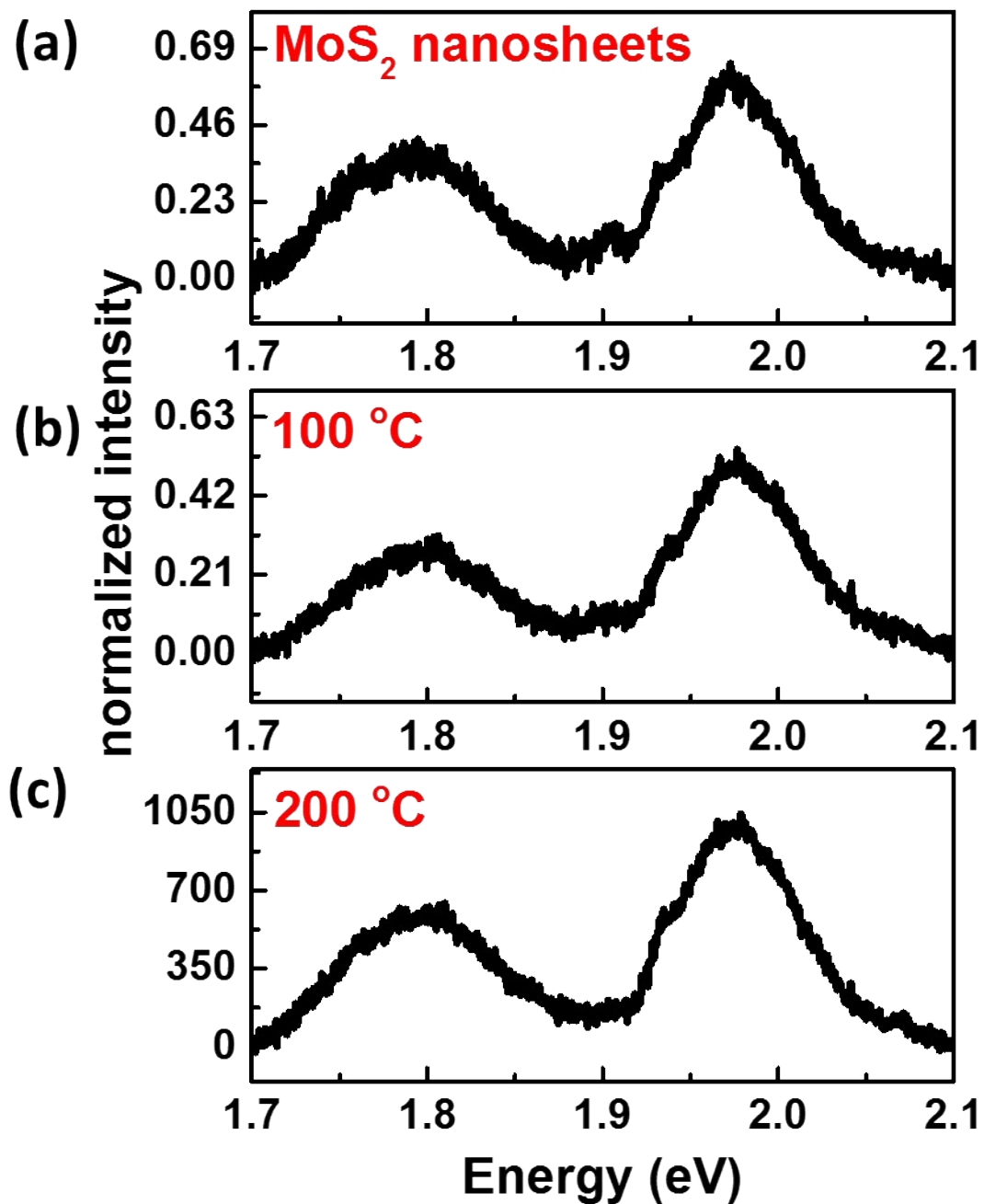


**Figure S20** PL spectra of (a) colloidal synthesized  $\text{MoS}_{2-x}$  and (b-c)  $\text{MoS}_{1.99}\text{Cu}_{0.01}$  with tetrakis(acetonitrile)copper (I) hexafluorophosphate decomposed at (b) 100 °C, and (c) 200 °C.

PL studies of  $\text{MoS}_{1.9}\text{Cu}_{0.1}$  synthesized at different temperature

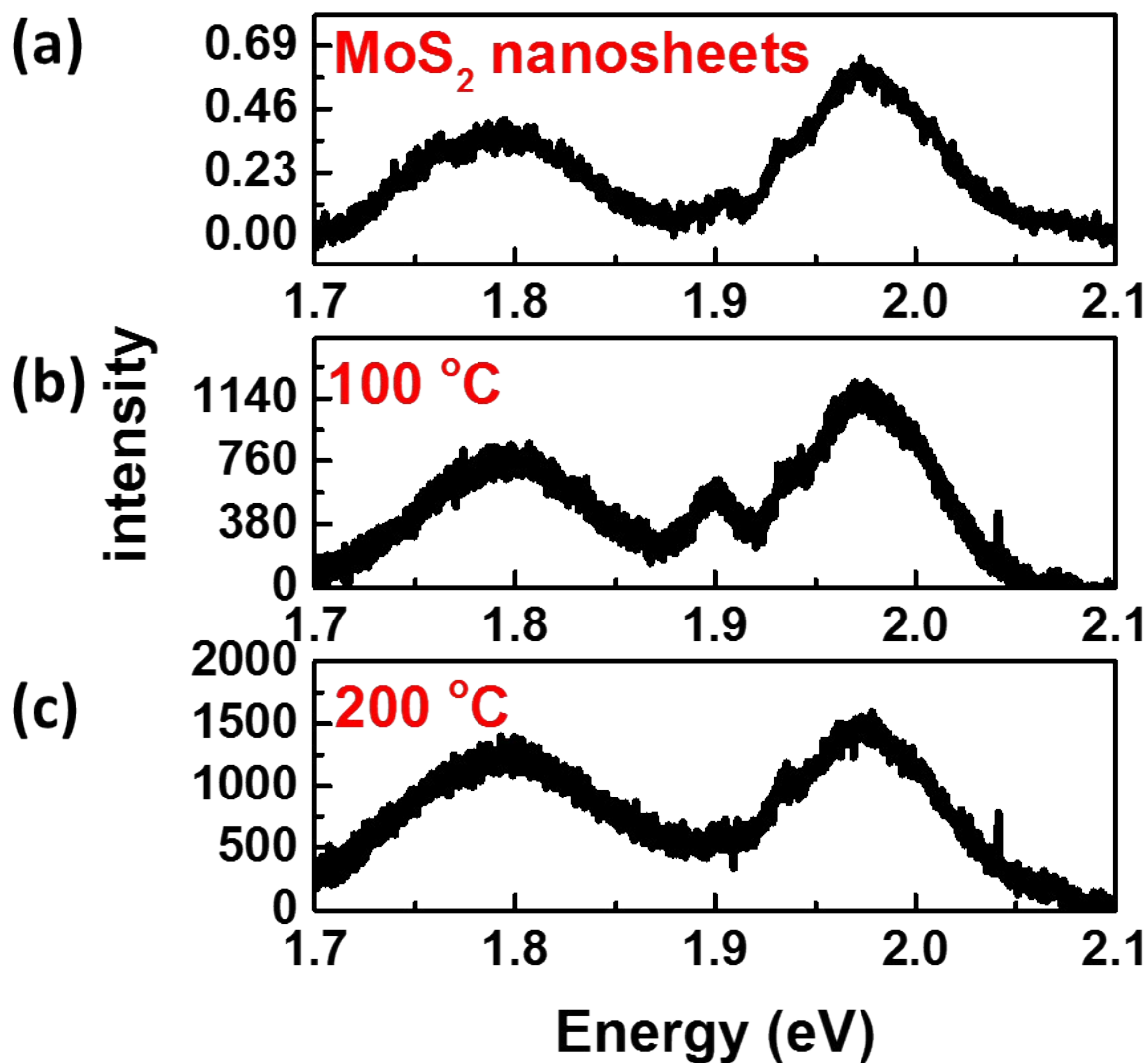


**Figure S21** PL spectra of (a) colloidal synthesized  $\text{MoS}_{2-x}$  and (b-d)  $\text{MoS}_{1.9}\text{Cu}_{0.1}$  with tetrakis(acetonitrile)copper (I) hexafluorophosphate decomposed at (b) 100 °C, and (c) 200 °C.

PL studies of  $\text{MoS}_1\text{Cu}_1$  synthesized at different temperature

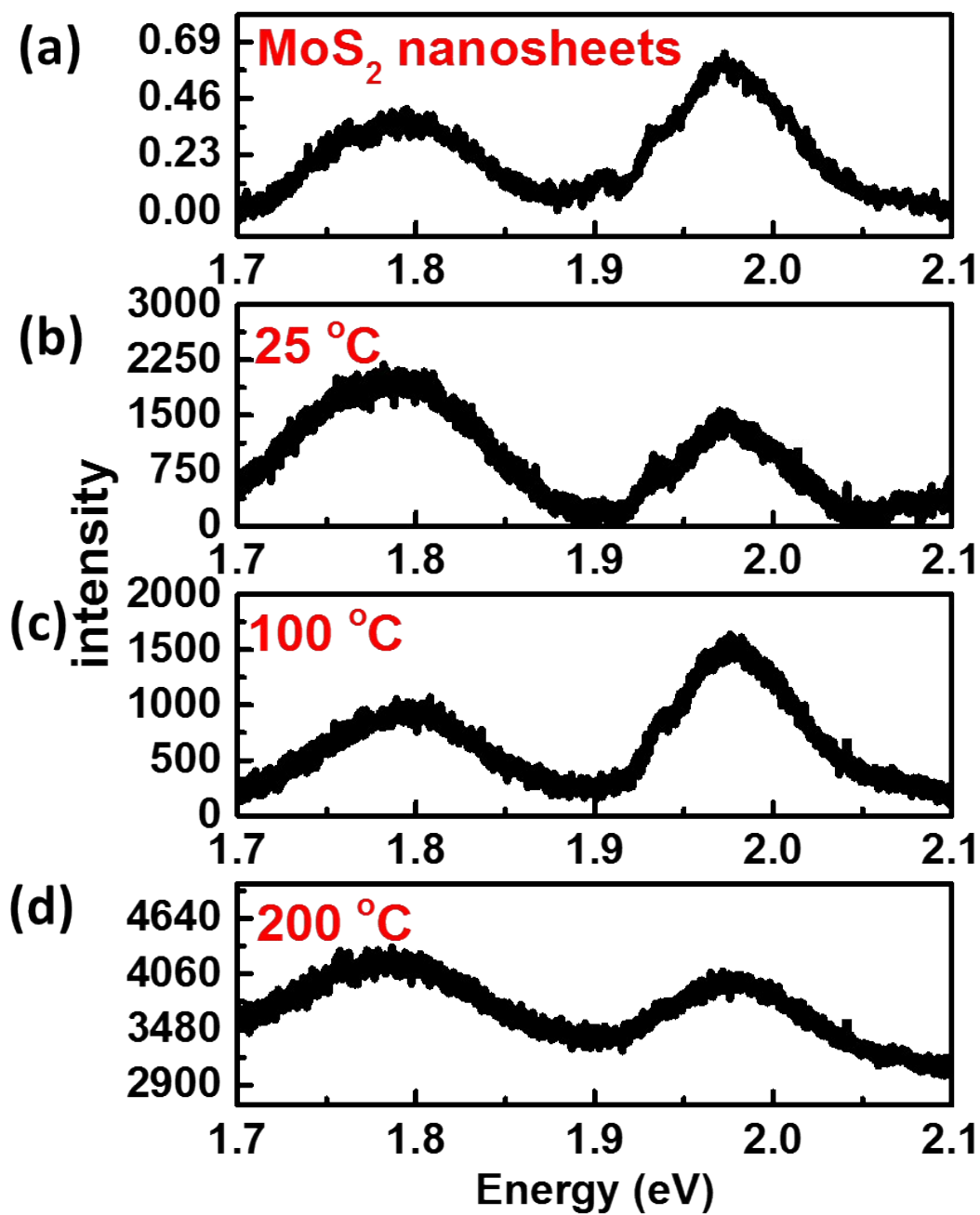


**Figure S22** PL spectra of colloidal synthesized (a)  $\text{MoS}_{2-x}$  nanostructures, (b-d)  $\text{MoS}_1\text{Cu}_1$  with tetrakis(acetonitrile)copper (I) hexafluorophosphate decomposed at (b)  $25\text{ }^\circ\text{C}$  (c)  $100\text{ }^\circ\text{C}$ , and (d)  $200\text{ }^\circ\text{C}$ .

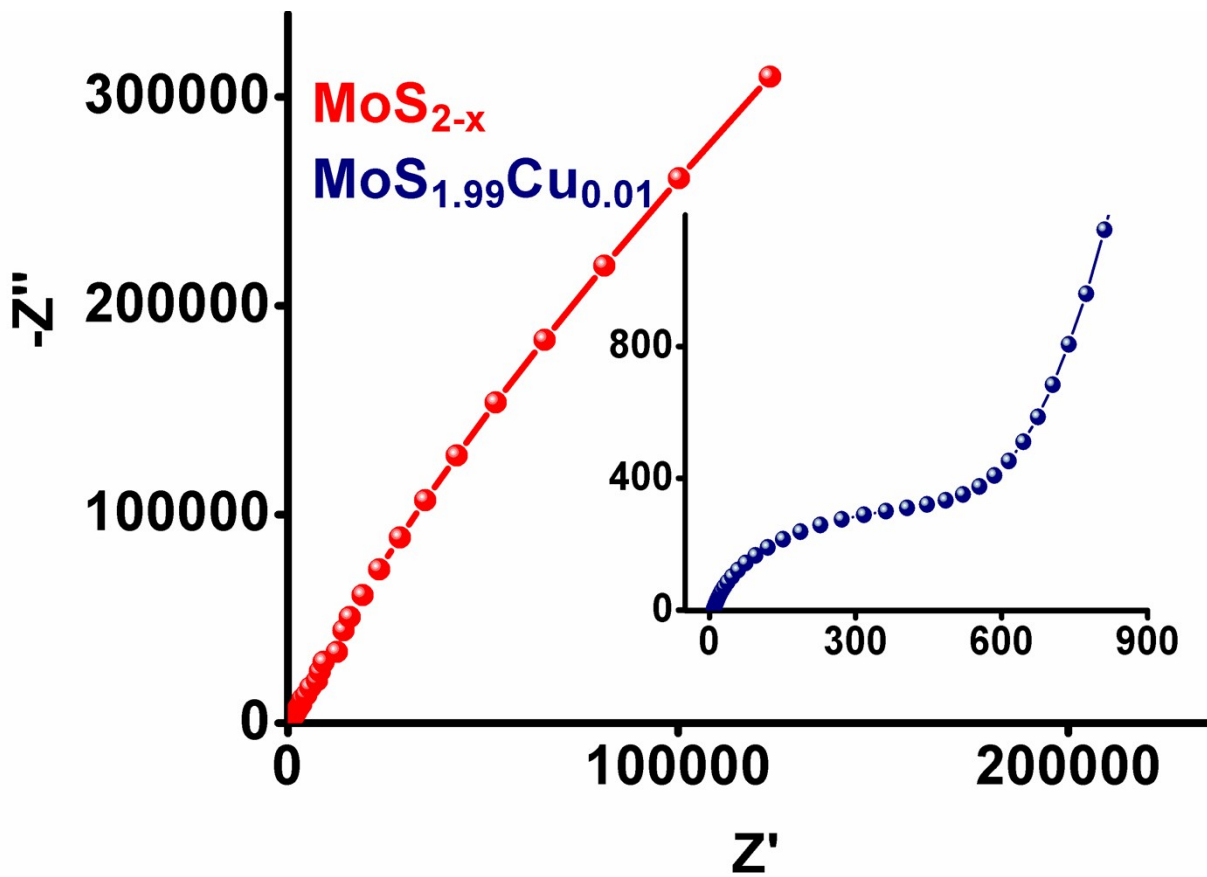


Figure S23. Nyquist plot of  $\text{MoS}_{2-x}$  and  $\text{MoS}_{1.99}\text{Cu}_{0.01}$

**Table S1** Molar ratio of copper oxide and molybdenum oxide to  $\text{MoS}_{2-x}\text{Cu}_x$  in the final product prepared under different reaction conditions.

<b>Sample</b>	<b>Cu Decomposition Temp (°C)</b>	<b>CuO: MoO<sub>3</sub>: MoS<sub>2-x</sub>Cu<sub>x</sub> (molar ratio)</b>
<b>MoS<sub>2</sub> nanostructures</b>	NA	0: 0.44: 1
<b>MoS<sub>1.99</sub>Cu<sub>0.01</sub></b>	100	0: 0.75: 1
<b>MoS<sub>1.9</sub>Cu<sub>0.1</sub></b>	100	0: 0.30: 1
<b>MoS<sub>1</sub>Cu<sub>1</sub></b>	100	0.07: 0.56: 1
<b>MoS<sub>1</sub>Cu<sub>1</sub></b>	200	0.12: 0.57: 1

**Table S2** Recent reports on catalytic performance of heteroatom-doped MoS<sub>2</sub>-based catalysts

<b>Dopant</b>	<b>Doping concentration (atomic %)</b>	<b>Onset potential [ <math>\eta</math>, mV]</b>	<b>Tafel slope (mV. dec<sup>-1</sup>)</b>	<b>Reference</b>
<b>Palladium</b>	1	-0.06	62	1
<b>Zinc</b>	4.33	-0.13	51	2
<b>Copper</b>	8.71	-0.16	68	2
<b>Nickel</b>	10.45	-0.19	89	2
<b>Iron</b>	10.77	-0.25	148	2
<b>Cobalt</b>	10.94	-0.24	141	3
<b>Nitrogen</b>	41	-0.3	77	4
<b>Copper</b>	<b>0.01</b>	<b>-0.26 (Initial cycle) -0.12 (After 1000 cycles)</b>	<b>75</b>	<b>Current work</b>

## References

- 1) Zhaoyan Luo, Yixin Ouyang, Hao Zhang, Meiling Xiao, Junjie Ge, Zheng Jiang, Jinlan Wang, Daiming Tang, Xinzhong Cao, Changpeng Liu & Wei Xing, chemically activating MoS<sub>2</sub> via spontaneous atomic palladium interfacial doping towards efficient hydrogen evolution, *Nat. Comm.* 2018, 9, 2120 (1-8).
- 2) Yi Shi, Jiong Wang, Chen Wang, Ting-Ting Zhai, Wen-Jing Bao, Jing-Juan Xu, Xing-Hua Xia, and Hong-Yuan Chen, Hot Electron of Au Nanorods Activates the Electrocatalysis of Hydrogen Evolution on MoS<sub>2</sub> Nanosheets, *J. Am. Chem. Soc.* 2015, 137, 7365-7370.
- 3) Congrong Wang, Shun Wang, Jianguo Lv, Yuxuan Ma, Yongqi Wang, Gaoliang Zhou, Mingsheng Chen, Min Zhao, Xiaoshuang Chen, Lei Yang, Co doped MoS<sub>2</sub> as Bifunctional Electrocatalyst for Hydrogen Evolution and Oxygen Reduction Reactions, *Int. J. Electrochem. Sci.*, 14 (2019) 9805-9814.
- 4) Qian Yang, Zegao Wang, Lichun Dong, Wenbin Zhao, Yan Jin, Liang Fang, Baoshan Hu, and Mingdong Dong, Activating MoS<sub>2</sub> with Super-High Nitrogen-Doping Concentration as, Efficient Catalyst for Hydrogen Evolution Reaction, *J. Phys. Chem. C* 2019, 123, 10917-10925